BMC Musculoskeletal Disorders

RESEARCH

Open Access

Comparative cross-sectional study of optimal screw positioning in the talus during arthroscopic ankle arthrodesis: a computed tomography-based analysis of talar bone density

Satoshi Kamijo[1*], Tsukasa Kumai[2] and Yasuhito Tanaka[3]

Abstract

Background To achieve successful osteosynthesis during arthroscopic ankle arthrodesis, increased stability and compression pressure during fixation are needed. Screw threads must be anchored within the talus, however, the bone mineral density of the talus has not been reported. This study used computed tomographic values to determine whether bone mineral density of the talus is lower in patients with ankle osteoarthritis than in healthy individuals and to determine the part of the talar cancellous bone with the highest bone mineral density.

Methods We studied the talus in 10 feet with and 10 without end-stage ankle osteoarthritis. Each talar cancellous bone was divided into the lateral process, head and neck, middle body, and medial body. Computed tomographic values of each segment were measured to calculate the relative bone mineral density difference between regions.

Results Mean (± standard deviations) computed tomographic values in the healthy talus group were 638.329 ± 139.765, 465.960 ± 74.254, 537.109 ± 82.443, and 469.016 ± 84.490 for the four segments. Mean computed tomographic values in the end-stage ankle osteoarthritis talus group were 360.994 ± 117.403, 284.397 ± 101.142, 327.814 ± 114.772, and 297.524 ± 105.667 for the same segments. The bone mineral density of the lateral process of the talus was significantly higher in both the healthy and osteoarthritis talus groups, and the bone mineral density of the talus in the osteoarthritis talus group was significantly lower than that in the healthy talus group.

Conclusions The bone mineral density of the talus in end-stage ankle osteoarthritis was significantly lower than that of a healthy talus. The highest relative bone mineral density was inferred to be from the middle body to the lateral process.

Keywords Computed tomographic value, Ankle osteoarthritis, Arthroscopic ankle arthrodesis, Talar fragility, Talar bone mineral density

*Correspondence:
Satoshi Kamijo
s.kamijo@kbh.biglobe.ne.jp
Full list of author information is available at the end of the article

© The Author(s) 2025. **Open Access** This article is licensed under a Creative Commons Attribution-NonCommercial-NoDerivatives 4.0 International License, which permits any non-commercial use, sharing, distribution and reproduction in any medium or format, as long as you give appropriate credit to the original author(s) and the source, provide a link to the Creative Commons licence, and indicate if you modified the licensed material. You do not have permission under this licence to share adapted material derived from this article or parts of it. The images or other third party material in this article are included in the article's Creative Commons licence, unless indicated otherwise in a credit line to the material. If material is not included in the article's Creative Commons licence and your intended use is not permitted by statutory regulation or exceeds the permitted use, you will need to obtain permission directly from the copyright holder. To view a copy of this licence, visit http://creativecommons.org/licenses/by-nc-nd/4.0/.

Background

The prevalence of osteoporosis increases from 2% in females aged 50 to >25% by 80 years [1]. An estimated one in five males >65 years sustains a fragile bone fracture [2]. Therefore, improved osteosynthesis methods are needed for enhanced stability required. Symptomatic ankle osteoarthritis (AOA) prevalence increases with age and worsens after age 50 and especially after age 70 [3, 4]. Therefore, AOA may be accompanied by osteoporosis, possibly with talar fragility. Ankle arthrodesis is the gold standard surgery for end-stage AOA [5–7], and bone fragility decreases arthrodesis construct stability [8]. Stability and compression are crucial during fixation to prevent postoperative nonunion in osteosynthesis instability between the tibial plafond and talar trochlea during ankle arthrodesis.

In open-ankle arthrodesis, residual cartilage and subchondral bone curettage can be performed under direct visual guidance [9], and joint surface conditions can be observed during arthrodesis. Firm fixation is confirmed by visually observing marrow juice gush when pressing bones together. However, in arthroscopic ankle arthrodesis, marrow juice gush cannot be directly observed and is indirectly confirmed via surgical imaging during osteosynthesis. Therefore, a more reliable fixation method is desirable for arthroscopic ankle arthrodesis.

The type of fixation device is important, and screw type affects crimping pressure and pressure change [10]. However, proper screw installation is crucial for achieving expected results; therefore, screw insertion must be optimized. Although screw insertion methods have been reported [11–16], the best screw thread location in the talar cancellous bone (TCB) remains unknown. As joint surface pressure after screw installation is caused by sandwiching the joint surface between the screw head and thread for typical cannulated cancellous screws, the screw thread location in the TCB is important for obtaining higher pressure. Inserting the screw thread into a part of the of the TCB with a higher BMD will be more advantageous for achieving bone fusion in arthroscopic ankle arthrodesis. Therefore, at least one cannulated cancellous screw is always inserted during fixation of arthroscopic ankle arthrodesis to position the threads in the lateral process (LP) of the TCB, as it is empirically inferred that it is the most solid. However, the bone mineral density (BMD) of each part of the TCB remains unknown. The study aimed to use computed tomography (CT) values to determine whether the BMD of the TCB is lower in patients with AOA than that in healthy individuals and to determine the part of the TCB with the highest BMD.

Materials and methods

Study participants

This study was approved by our ethics committee. Written informed consent was obtained from all the participants. Ten taluses from patients without a history of AOA or ankle complaints requiring CT imaging for other diseases (healthy talus group; two male and eight female, mean ± SD age 58.4 ± 11.8 years, and BMI 23.2 ± 2.29 kg/m^2) and 10 taluses from patients with end-stage AOA (Takakura Classification IIIb-IV) scheduled for arthroscopic ankle arthrodesis (AOA talus group; one male and nine female, mean ± SD age 66.9 ± 9.54 years, and BMI 24.9 ± 2.89 kg/m^2) were included. The study spanned 12 months, enrolling consecutive patients as they visited the hospital and provided consent. Diagnosis of AOA was confirmed by the author (an orthopedic surgery specialist) and an independent orthopedic surgery specialist. Imaging was performed using a 64-row multi-slice CT instrument (Discovery Optima CT 660, GE Healthcare Japan, Tokyo, Japan) with a slice thickness of 1 mm and a tube voltage of 120 kV. Morphological operation software (SYNAPSE VINCENT, FUJIFILM Medical Co., Ltd., Tokyo, Japan) was used to exclude areas corresponding to the talar cortex from the images, isolating the TCB (Fig. 1). The TCB was subsequently divided into the following four segments based on fixed criteria: the lateral side of the body (LP), head and neck (HN), middle of the body (MIB), and medial body (MEB) (Fig. 2a). CT value calculation software (SYNAPSE VINCENT, FUJIFILM

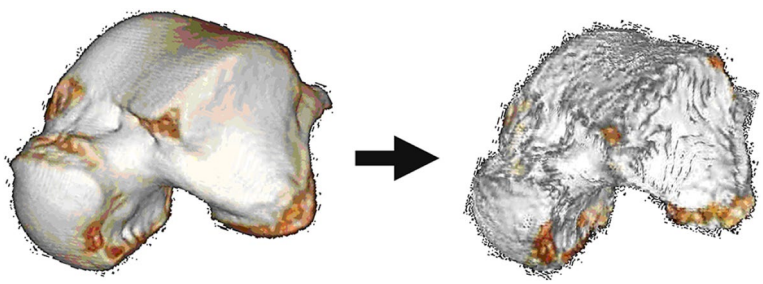

Fig. 1 Removing areas corresponding to the talus cortex from images via morphological image processing

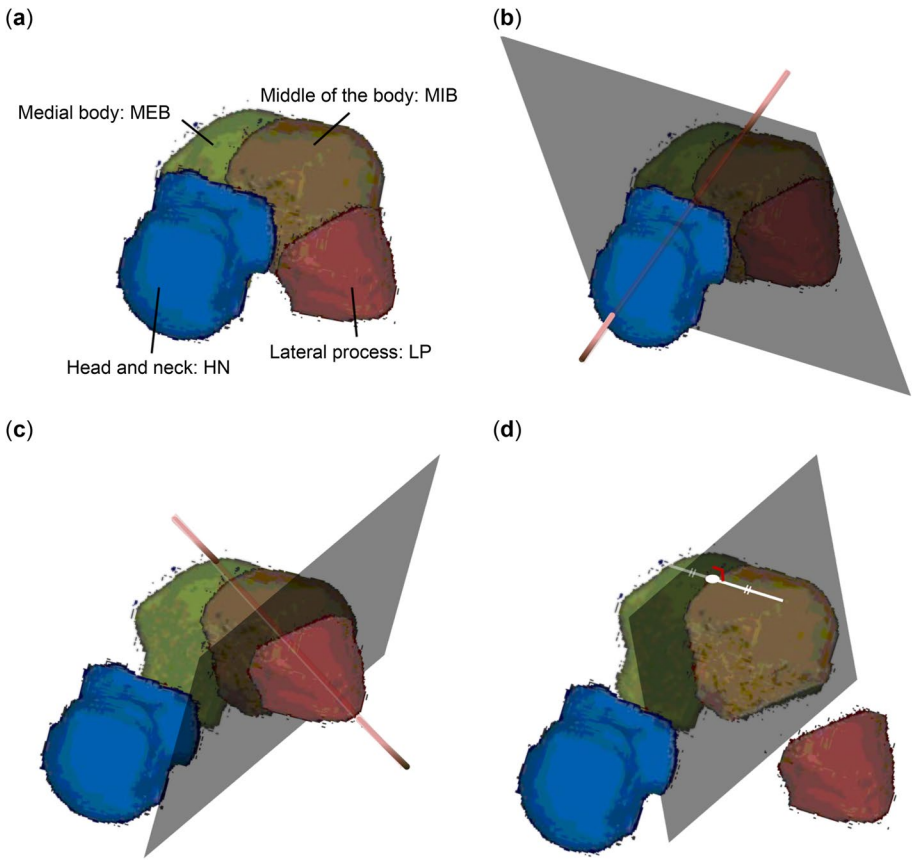

Fig. 2 **a** TCB into the following four segments according to fixed criteria: LP (lateral side of the body), head and neck (HN), middle of the body (MIB), and medial body (MEB). **b** HN segment is separated by the plane in contact with the anterior border of the talar trochlea and perpendicular to the talar neck axis. **c** The LP segment is separated by the plane that passes the point where articular surface curvature of the talar lateral malleolus begins and is perpendicular to the straight line connecting the two points; the apex of the medial border of the trochlea and the outermost end of the LP of the talus. **d** Each segment of the MIB and MEB is divided by the plane perpendicular to the line segment connecting the apexes of the medial and lateral borders of the trochlea and passing through the midpoint of the line segment

Medical Co., Ltd., Tokyo, Japan) was used to compare the average Hounsfield units ($[HU]_{ave.}$). obtained from these regions.

Criteria for dividing the TCB into segments

1) The HN segment separated by a plane perpendicular to the talar neck axis, in contact with the anterior border of the trochlea (Fig. 2b).
2) The LP segment separated by a plane passing through the point where the articular surface curvature of the talar lateral malleolus begins and is perpendicular to the straight line connecting the apex of the medial border of the trochlea and the outermost end of the LP of the talus (Fig. 2c).
3) MIB and MEB segments divided by a plane perpendicular to the line segment connecting the apexes of the medial and lateral borders of the trochlea, passing through the midpoint of that line segment (Fig. 2d).

The $[HU]_{ave.}$ of each part of each talar sample was calculated using the following formula:

$$[HU]_{ave.} = \frac{\sum([HU] \times V_{[HU]})}{V_{all}}$$

where the CT value is given in [HU], the volume at which the CT value is $V_{[HU]}$, and the volume of each segment is V_{all} (Fig. 3).

Statistical analyses

Statistical analyses were performed using The Bell Curve in Excel version 4.07 software (Social Survey Research Information Co., Ltd., Tokyo, Japan) by corresponding author. The Kolmogorov–Smirnov test was used to test for normality. Differences between sections were

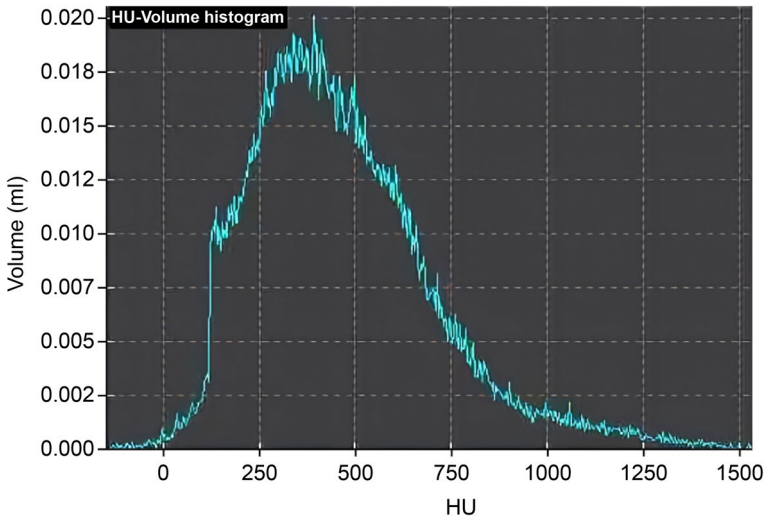

Fig. 3 Example of HU–Volume histogram of part of the talus

identified using one-way repeated-measures analysis of variance and Holm's multiple comparison test. All tests were two-tailed. Data are presented as the mean and standard deviation (SD). Values of $p < 0.05$ were indicative of statistically significant differences, with an (*) indicating $0.01 \leq p < 0.05$, (**) indicating $0.001 \leq p < 0.01$, and (***) indicating $p < 0.001$.

Results

Normality was confirmed for all datasets using the Kolmogorov–Smirnov test. There were no significant differences between the healthy talus group and the AOA talus group in male/female ratio, mean age, and mean BMI ($p = 0.531$, 0.068, and 0.309, respectively).

The mean CT values ($[HU]_{ave.}$) of LP, HN, MIB, MEB of the healthy talus group were 638.329 ± 139.765 SD, 465.960 ± 74.254 SD, 537.109 ± 82.443 SD, and 469.016 ± 84.490 SD, respectively. The $[HU]_{ave.}$ values were significantly higher for the LP than for other segments of the talus ($p < 0.01$). The $[HU]_{ave.}$ values were significantly higher for MIB than those for HN and MEB ($p < 0.05$) (Fig. 4a).

The $[HU]_{ave.}$ values in the AOA talus group were 360.994 ± 117.403 SD, 284.397 ± 101.142 SD, 327.814 ± 114.772 SD, and 297.524 ± 105.667 SD for the LP, HN, MIB, and MEB, respectively. The $[HU]_{ave.}$ value was significantly higher for the LP than that for HN and MEB ($p < 0.01$); however, it was not significantly different from that of MIB. The $[HU]_{ave.}$ value was significantly higher for MIB than that for HN ($p < 0.05$), and no significant difference was observed between the $[HU]_{ave.}$ values of HN and MEB (Fig. 4b).

When the $[HU]_{ave.}$ values were compared between the healthy and AOA talus groups, $[HU]_{ave.}$ values for all segments were significantly lower in the AOA talus group ($p < 0.001$) (Fig. 4c).

Discussion

In previous studies on screw insertion in arthroscopic ankle arthrodesis, there has been much discussion about the site and direction of screw insertion to achieve joint surface stabilization during fixation [11–16]. However, in our knowledge, no study has focused on the BMD of the talus for screw insertion to achieve joint surface stabilization during fixation which is one of the important factors for bone union.

Bone strength is primarily determined by BMD, accounting for approximately 70% of bone strength [17, 18]. A positive correlation exists between BMD and CT values [19, 20]. Accordingly, identifying high BMD areas using CT values allowed us to achieve stronger fixation by targeting these areas for screw insertion. Lee et al. found CT values useful for differentiating patients with osteoporosis from healthy individuals [21]. In our study, CT values were significantly lower in the in the talar AOA group, requiring arthroscopic ankle arthrodesis, than those in the healthy talus group, indicating low BMD. Therefore, for the talar AOA group, optimizing screw insertion methods and insertion placement is crucial for improving fixation reliability during arthroscopic ankle arthrodesis. As the TCB volume for screw placement is limited, making it difficult to insert a numerous screws, it is important to devise methods to obtain effective pressure fewer screws. Our results showed higher CT values in the LP than those in the

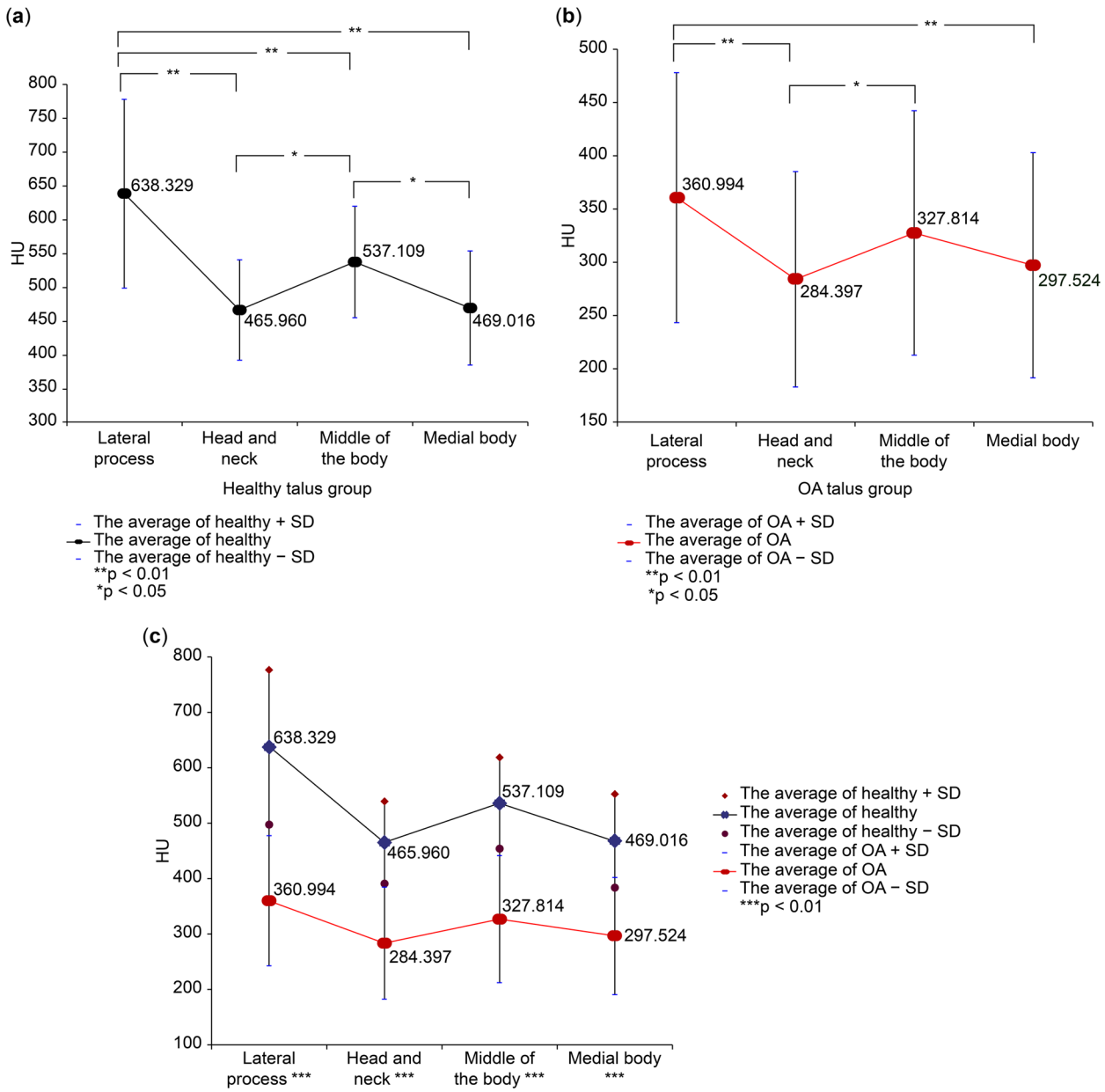

Fig. 4 **a** $[HU]_{ave.}$ values of LP, HN, MIB, and MEB of the healthy talus group; $[HU]_{ave.}$ values were significantly higher for LP than that for other segments of the talus. Additionally, the $[HU]_{ave.}$ values were significantly higher for MIB than for HN and MEB. **b** $[HU]_{ave.}$ values in the AOA talus group for the respective LP, HN, MIB, and MEB segments; the $[HU]_{ave.}$ value was significantly higher for LP than that for HN and MEB; however, it was not significantly different from that of MIB. $[HU]_{ave.}$ value was significantly higher for MIB than that for HN, and no significant difference was observed between $[HU]_{ave.}$ values of HN and MEB. **c** Comparing $[HU]_{ave.}$ values between the healthy and AOA talus groups; $[HU]_{ave.}$ values of all segments were significantly lower in the AOA talus group

HN and MEB in both healthy and AOA talus groups. In addition, talar AOA cases, which is an indication for surgical treatment, CT values were higher for the LP, although no significant difference was observed between the LP and MIB. We concluded that the BMD of the TCB was higher in the LP and MIB than that in the HN and MEB. Therefore, at least one screw should have its thread positioned in the LP, inserted from above the medial malleolus toward the LP, as shown in Fig. 5. However, the LP has a narrower area than the other parts, making it difficult to position a second or third thread there. The MEB has the lowest CT value, indicating the lowest BMD, making it disadvantageous for initiating the positioning of screw threads in terms

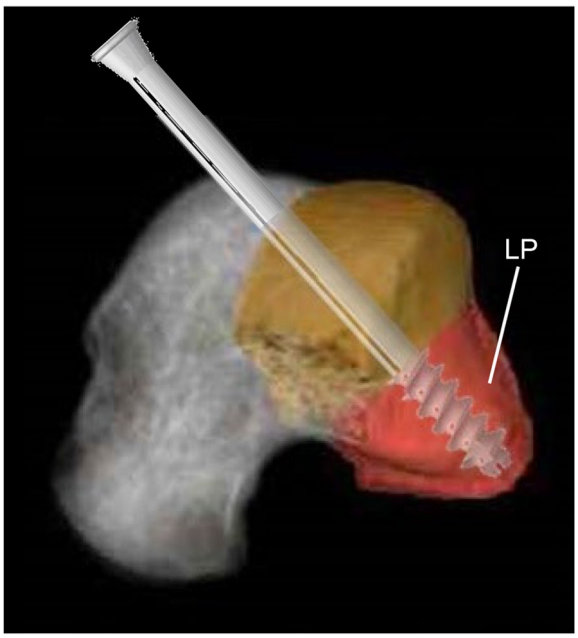

Fig. 5 Screw inserted from above the medial malleolus toward the LP

of compression pressure. Reports of screw insertion from the lateral side of the tibia toward the MEB [11, 13] suggest this method is suboptimal for compression pressure. Therefore, for maximum compression pressure, the second and third screws should be inserted above the medial malleolus, with threads positioned in the MIB. However, in cases requiring biomechanical stability or when anterior subluxation of the talus is present (common in end-stage AOA) [22, 23], cross-screwing [11, 13], and/or home run screw techniques [16] are highly effective. Therefore, adding a screw thread in the LP alongside these techniques enhances biomechanical stability and fixation can by providing higher compression pressure.

A limitation of this study is the relatively small sample size, which may limit the generalizability of the findings. However, the absence of prior studies and power analysis made determining an appropriate sample size difficult. Ethical considerations will guide further efforts to increase the sample size to assess whether similar results are obtained. Another limitation is the study's assumption of a general cannulated cancellous screw (with head and tip thread) rather than a headless screw, such as the Acumed® Acutrak® screw, necessitating future comparisons of crimping pressure performance between these screw types. Furthermore, additional limitations arise from the lack of clinical studies, such as the need to compare outcomes of arthroscopic ankle arthrodesis with and without screw thread in the LP.

Conclusions

The BMD of the talus in patients with end-stage AOA was significantly lower than that in healthy talus. The highest relative BMD was observed from the middle of the body to the LP. Therefore, for optimal compression pressure during screw insertion in arthroscopic ankle arthrodesis, at least one screw thread should be positioned in the LP. Future studies have been planned to support our claims based on clinical data.

Abbreviations

AOA	Ankle osteoarthritis
BMD	Bone mineral density
CT	Computed tomography
HN	Head and neck
LP	Lateral process
MEB	Medial body
MIB	Middle of the body
TCB	Talar cancellous bone

Acknowledgements

The authors thank the Department of Radiology, Fujimori Hospital (Matsumoto, Nagano Prefecture, Japan) for providing experimental instruments, software, and advice. We would like to thank Editage (www.editage.jp) for English language editing.

Authors' contributions

SK and TK conceived and designed the study. TK and YT provided study design advice, supervision, and project administration. SK performed experiments, analyzed data, and wrote the manuscript. All authors have read and approved the final submitted manuscript.

Funding

Not applicable.

Data availability

The datasets used and/or analysed during the current study are available from the corresponding author on reasonable request. The data are not publicly available owing to privacy concerns.

Declarations

Ethics approval and consent to participate

All procedures involving human participants adhered to the ethical standards of the institutional and/or national research committee and the 1964 Helsinki Declaration and its amendments. This study approved by the Ethics Committees of Fujimori Hospital (approval no. 0025001). Written informed consent was obtained from all participants.

Consent for publication

Not applicable.

Competing interests

The authors declare no competing interests.

Author details

[1]Center for Foot and Ankle Surgery & Department of Orthopedic Surgery, Suwakohan Hospital, 1-11-30 Osachi Kohagi, Okaya, Ngano 394-8515, Japan. [2]Faculty of Sport Sciences, Waseda University, 2-579-15, Mikajima, Tokorozawa, Saitama 359-1192, Japan. [3]Department of Orthopaedic Surgery, Nara Medical University, 840 Shijyo-Cho, Kashihara, Nara 634-8522, Japan.

Received: 2 January 2025 Accepted: 22 May 2025
Published online: 29 May 2025

References

1. Rabar S, Lau R, Oflynn N, Li L, Barry P, Guideline Development Group. Risk assessment of fragility fractures: summary of NICE guidance. BMJ. 2012;345:e3698. https://doi.org/10.1136/bmj.e3698.
2. Piccirilli E, Cariati I, Primavera M, Triolo R, Gasbarra E, Tarantino U. Augmentation in fragility fractures, bone of contention: a systematic review. BMC Musculoskelet Disord. 2022;23:1046. https://doi.org/10.1186/s12891-022-06022-0.
3. Murray CL, Marshall M, Rathod T, Menz H, Roddy E. Population prevalence and distribution of ankle pain and symptomatic radiographic ankle osteoarthritis in community-dwelling older adults. Rheumatology. 2016;1:79. https://doi.org/10.1093/rheumatology/kew140.006.
4. Nishimura A, Senga Y, Fujikawa Y, Takegami N, Akeda K, Ogura T, et al. Prevalence and risk factors of ankle osteoarthritis in a population-based study. Foot Ankle Surg. 2024;30.5:389-93. https://doi.org/10.1016/j.fas.2024.02.009.
5. Nogod S, Khairy AMM, Nubi OG, Fatooh MS, Abd-Elmaged HM. Ankle arthrodesis: Indications, outcomes, and patient satisfaction. Cureus. 2023;15:e37177.
6. Van Den Heuvel SBM, Penning D, Schepers T. Open ankle arthrodesis: A retrospective analysis comparing different fixation methods. J Foot Ankle Surg. 2022;61:233–8. https://doi.org/10.1053/j.jfas.2021.07.012.
7. Bai Z, Yang Y, Chen S, Dong Y, Cao X, Qin W, et al. Clinical effectiveness of arthroscopic vs open ankle arthrodesis for advanced ankle arthritis: a systematic review and meta-analysis. Medicine. 2021;100:e24998. https://doi.org/10.1097/MD.0000000000024998.
8. Wirth AJ, Müller R, van Lenthe GH. The discrete nature of trabecular bone microarchitecture affects implant stability. J Biomech. 2012;456:1060–7. https://doi.org/10.1016/j.jbiomech.2011.12.024.
9. Lorente A, Pelaz L, Palacios P, Bautista IJ, Mariscal G, Barrios C, et al. Arthroscopic vs. open-ankle arthrodesis on fusion rate in ankle osteoarthritis patients: a systematic review and meta-analysis. J Clin Med. 2023;12:3574. https://doi.org/10.3390/jcm12103574.
10. Kamijo S, Kumai T, Tanaka S, Mano T, Tanaka Y. Comparison of compressive forces caused by various cannulated cancellous screws used in arthroscopic ankle arthrodesis. J Orthop Surg Res. 2017;12:7. https://doi.org/10.1186/s13018-016-0503-x.
11. Vaishya R, Azizi AT, Agarwal AK, Vijay V. Arthroscopic assisted ankle arthrodesis: a retrospective study of 32 cases. J Clin Orthop Trauma. 2017;8:54–8. https://doi.org/10.1016/j.jcot.2016.12.002.
12. Elmlund AO, Winson IG. Arthroscopic ankle arthrodesis. Foot Ankle Clin. 2015;20:71–80. https://doi.org/10.1016/j.fcl.2014.10.008.
13. Goetzmann T, Mole D, Jullion S, Roche O, Sirveaux F, Jacquot A. Influence of fixation with two vs. three screws on union of arthroscopic tibio-talar arthrodesis: comparative radiographic study of 111 cases. Orthop Traumatol Surg Res. 2016;102(5):651–6. https://doi.org/10.1016/j.otsr.2016.03.015.
14. Yoshimura I, Kanazawa K, Takeyama A, Ida T, Hagio T, Angthong C, et al. The effect of screw position and number on the time to union of arthroscopic ankle arthrodesis. Arthroscopy. 2012;28:1882–8. https://doi.org/10.1016/j.arthro.2012.06.019.
15. Lee MS. Arthroscopic ankle arthrodesis. Clin Podiatr Med Surg. 2011;28:511–21. https://doi.org/10.1016/j.cpm.2011.04.008.
16. Wang S, Yu J, Ma X, Zhao D, Geng X, Huang J, et al. Finite element analysis of the initial stability of arthroscopic ankle arthrodesis with three-screw fixation: posteromedial versus posterolateral home-run screw. J Orthop Surg Res. 2020;15:1–9. https://doi.org/10.1186/s13018-020-01767-7.
17. Hart NH, Nimphius S, Rantalainen T, Ireland A, Siafarikas A, Newton RU, et al. Mechanical basis of bone strength: influence of bone material, bone structure and muscle action. J Musculoskelet Neuronal Interact. 2017;17(3):114.
18. Rizzoli R. Postmenopausal osteoporosis: assessment and management. Best Pract Res Clin Endocrinol Metab. 2018;32(5):739–57. https://doi.org/10.1016/j.beem.2018.09.005.
19. Bartenschlager S, Cavallaro A, Pogarell T, Chaudry O, Uder M, Khosla S, et al. Opportunistic screening with CT: Comparison of phantomless BMD calibration methods. J Bone Miner Res. 2023;38:1689–99. https://doi.org/10.1002/jbmr.4917.
20. Kang J-W, Park C, Lee D-E, Yoo J-H, Kim M. Prediction of bone mineral density in CT using deep learning with explainability. Front Physiol. 2022;13:1061911. https://doi.org/10.3389/fphys.2022.1061911.
21. Lee H, Park S, Kwack K-S, Yun JS. CT and MR for bone mineral density and trabecular bone score assessment in osteoporosis evaluation. Sci Rep. 2023;13:16574. https://doi.org/10.1038/s41598-023-43850-z.
22. Tomiwa K, Tanaka Y, Kurokawa H, Kadono K, Taniguchi A, Maliwankul K. Simulated weightbearing computed tomography for verification of radiographic staging of varus ankle osteoarthritis: a cross-sectional study. BMC Musculoskelet Disord. 2021;22:737. https://doi.org/10.1186/s12891-021-04618-6.
23. DiStefano JG, Stephen P. Ankle arthritis: etiology and epidemiology. Semin Arthroplasty. 2010;21(4):218–22. https://doi.org/10.1053/j.sart.2010.09.002.

Publisher's Note

Springer Nature remains neutral with regard to jurisdictional claims in published maps and institutional affiliations.